J Mater Sci (2010) 45:5257–5263
DOI 10.1007/s10853-010-4568-3

A calcium phosphate cryogel for alkaline phosphatase encapsulation

Peih Jeng Jiang · Gareth Wynn-Jones · Liam M. Grover

Received: 24 December 2009 / Accepted: 27 April 2010 / Published online: 20 May 2010

Abstract There has been significant interest in the development of biomaterials that can localise drugs, enzymes and other therapeutic molecules and be well tolerated in the body. To date, the majority of research in this area has focussed on the formulation and refinement of silica-based gels. Whilst significant progress has been made in optimising silica gel materials, their manufacture typically requires the use of toxic precursors. Here we report the encapsulation of alkaline phosphatase (ALP) in a calcium phosphate-based cryogel. The activity of the ALP following encapsulation, over a period of 14 days, was evaluated and compared with the activity of horseradish peroxidise (HRP), a model enzyme often used in encapsulation studies. Furthermore, the chemical and structural properties exhibited by the gel were determined using X-ray diffraction, helium pycnometry and mercury porosimetry. It was found that when encapsulated in the gel, the activity of ALP was preserved and remained higher than when aged for an equivalent amount of time free in solution. In the case of HRP, however, encapsulation reduced enzyme activity. This was attributed to the different sizes and charges exhibited by the substrates of these two enzymes and the associated diffusional limitations through the mesopores of the gel structure.

Introduction

The sol–gel process has been used for the encapsulation of biomolecules in biosensors, and to produce carriers for the delivery of therapeutic molecules in reparative medicine [1]. Silica gels, for example, have been successfully used for the encapsulation of horseradish peroxidase (HRP). They are, however, traditionally made using tetraethyl orthosilicate (TEOS) or tetramethoxy silane (TMOS), which have been shown to be toxic and can reduce enzyme activity [2, 3]. Consequently, rather than using TEOS or TMOS, some researchers have used sodium silicate precursors. Although this may have solved issues related to the toxicity of the sol–gel, loading efficiency was shown to be low [4, 5]. Efforts have also been made to enhance enzyme activity by the addition of polymers, dendrimers and sugars into the matrix of silica sol–gels with limited success [6–9].

Although silica-based materials have been shown to be tolerated in vivo, the use of toxic reactants and the dissimilarity of the composition to that of hard tissue, means that they could not form a significant bond with hard tissues [10]. In comparison, calcium phosphate-based ceramic materials have been used as hard tissue replacements and prosthesis coatings for several decades [11]. Since they have a similar composition to the mineral component of bone, they are well tolerated in the body and form a little understood bond with both hard and soft tissues [12]. Traditionally, calcium phosphate-based ceramics were made by a high temperature process, which precluded the incorporation of temperature sensitive therapeutic proteins during manufacture. The subsequent development of calcium phosphate-based cement (CPC) materials [13], which set in ambient conditions, allowed the delivery of proteins such as bone morphogenic protein [14] and transforming growth factor β [15]. Although CPCs have been successfully used as a carrier of therapeutic compounds [16, 17], the macroporous structure (10–100 μm) of the hardened product has restricted their use for the encapsulation of enzymes. By forming hydroxyapatite using a precipitation

P. J. Jiang · G. Wynn-Jones · L. M. Grover (✉)
School of Chemical Engineering, University of Birmingham, Edgbaston B15 2TT, UK
e-mail: l.m.grover@bham.ac.uk; liam.grover@gmail.com

reaction, it is possible to manipulate process conditions to form a calcium phosphate-based sol–gel [18]. In common with the cement hardening reaction, these sol–gel materials are formed in ambient conditions and with relatively little pH fluctuation. What gives them an important advantage over CPCs is that by controlling the rate of removal of the liquid phase, it is impossible to exercise some form of control over pore size, thus enabling control over release rate. A previous study [18] has shown that apatite-based gels can store proteins such as albumin for a period of 52 weeks in vitro with little undesired release from the matrix.

Alkaline phosphatase (ALP) is one enzyme that has been encapsulated in glass, ceramic and polymeric matrices, as well as being immobilised on the surface of metallic implants [19, 20]. ALP has been investigated widely as it has been implicated with the mineralisation of newly forming bone [21]. Indeed, tissue non-specific ALP is found on the surface of osteoblast membranes and is present in high concentrations in the matrix vesicles excreted from these cells during the mineralisation process [22]. A recent study has shown that ALP functions by removing pyrophosphate ions, potent inhibitors of hydroxyapatite crystal formation, which creates localised supersaturation with respect hydroxyapatite and crystal deposition [23]. ALP has previously been encapsulated in TMOS-based silica gels, although the activity of the encapsulated ALP was shown to be relatively low [24]. Other studies have shown that encapsulation of ALP in silica-based sol–gels could preserve activity, even during storage in acidic environments [25]. In previous studies, relatively low ALP activity has been proposed to be as a result of poor mass transport through the mesoporous gel systems, low loading efficiencies and enzyme desorption. Attempts have been made to address the mass transport problem, through the incorporation of bimodal pore size distributions (2–3 nm/10–40 nm) [26]. Here, we evaluate the use of a calcium phosphate-based cryogel material for the encapsulation of ALP. The activity of the ALP was evaluated over a period of 14 days and compared with the activity of HRP, a model enzyme often used for evaluating the efficacy of encapsulation. The influence of protein incorporation into the calcium phosphate matrix during fabrication on the composition and pore structures of the gel material were evaluated.

Methods and materials

The apatite cryogels (ACGs) were formed in accordance with the method of Barralet et al. [18]. An equal volume of 130 mM triammonium orthophosphate (Rose Chemicals, London, UK) and 320 mM sodium hydrogen carbonate (Fisher scientific, Loughborough, UK) were added into an equal volume of 210 mM calcium acetate (Sigma-Aldrich, Gillingham, UK) which was adjusted to pH 12 using ammonium hydroxide (Sigma-Aldrich, Gillingham, UK). The resulting precipitate was then stirred for 12 h in ambient conditions, following which, the pH of the precipitate was adjusted to pH 7.4 using concentrated HCl (Sigma-Aldrich, Gillingham, UK). For the control material, the precipitate was then filtered using a water aspirated vacuum and dried in a freeze drier (Edwards, Sussex, England). For HRP encapsulation, HRP (169 units mg^{-1}, Sigma Chemical Co., Germany) was mixed with the ACGs in the ratio 800 mg ACGs: 2 mg HRP. The mixture was then homogenised within a nitrile mixing vessel (Kimberly-Clark, Rosewell, USA) resulting in ACG containing 0.25 wt% HRP. After the HRP had been loaded into the samples, the gels were then dried in a vacuum at −20 °C (Edwards, Sussex, England). For ALP encapsulation 1.46 units mg^{-1} of ALP (Fluka, Gillingham, UK) were mixed with ACGs in the ratio 97 g ACGs: 3 g ALP. The mixture was then homogenised for 15 min in a nitrile mixing vessel and the resulting apatite slurry containing 3 wt% ALP was filtered using a water aspirated vacuum pump before freeze drying.

The crystalline compositions of ACGs were determined using Cu–Kα radiation from a Ge primary beam monochromator, at a scanning rate of 1°2θ min^{-1} from 5° to 60° 2θ (D5000, Siemens-Nixdorf, Münich, Germany). Carbonate substitution of ACGs was evaluated using an absorbance FTIR spectrum (NICOLET 380, Thermo Electron, Madison, USA) at a spatial resolution of 1.929 cm^{-1} and 32 scans. The micro-porosity of ACGs was analysed using a mercury porosimeter (AutoPore IV 9500, Micromeritics, USA). Briefly, 1 g of ACG was loaded into a penetrometer (920-61710-01, 5c.c., Micromeritics, USA) before measurement, the ACG was dehydrated in a desiccator with a vacuum pump. The particle size of the ACGs was measured using a high performance particle sizer MS2000 (Malvern Instruments Ltd., Malvern, UK) at 25 °C. The sample was prepared by dispersing 1 mg of the ACG powder in 100 mL of distilled water. Samples were treated for 15 min with ultrasound prior to measurement. As a visual measure of particle size, transmission electron microscopy (TEM) was used to evaluate a dispersed sample (FEI Philips TECNAI F20, Oregon, USA), prepared by dispersing the ACGs into the distilled water, and placing the resulting dispersion onto a 200 mesh. The resulting sample was examined at an accelerating voltage of 200 kV. The surface characteristics of the ACG were evaluated using a scanning electron microscope (FEI Philips XL30 ESEM-FEG, Oregon, USA). To determine true density, dried ACGs were placed into a helium pycnometer (ACCU-PYC

II 1340, Micromeritics, USA) and were subject to ten purges with He prior to ten volume measurements. The specific surface areas exhibited by the ACGs were determined by applying the Brunauer Emmet Teller (BET) equation to data collected using a dynamic vapour sorption (DVS) system (Advantage II, Surface Measurement Systems, Middlesex, UK) using octane as the probe molecule.

The amount of protein released from the ACGs with ALP/HRP was determined by using the BCA assay. According to the amount of reduction of the Cu^{2+} to Cu^{+} by protein, the protein can be quantified by monitoring the cuprous cation, using a UV–Vis spectrophotometer at 562 nm. The calibration curve consisted of a known concentration of bovine serum albumin (BSA) between 0 and 1000 μg mL^{-1}. The blank was made of a phosphate buffer with no enzyme. 100 μL of a sample/blank was mixed with 2 mL of the BCA working reagent. Then, the solution was incubated in the 37 °C incubator for 30 min. ACGs loaded with HRP (n = 3) were immersed in 10 mL of 100 mM KH_2PO_4 buffered (pH 6) over a week, and control ACGs were immersed in an identical process. All samples were placed in a horizontally rotating shaker at 90 rpm in a 37 °C environment. At selected time points between 0.5 and 216 h observations were made by collecting all released medium and refreshing the buffer after each withdrawal from the HRP and ACGs. Then the absorbance of the ABTS cation at 414 nm and the activity of HRP were measured. ACGs loaded with ALP (n = 3) were immersed in 5 mL of 100 mM Tris–HCL buffer (pH 7.4) over a week, and control ACGs were immersed in an identical process.

The activity of HRP was measured based on the oxidation of 30 μM ABTS catalysed by 2 mg HRP loaded into ACGs in the presence of 9.79 μM H_2O_2 to the ABTS cation. The interconversion of ABTS to its radical cation was monitored using a UV–Vis spectrophotometer (UVIKON 922, Northstar Scientific, Potton, UK) as a function of time. The formation of ABTS cation indicated the HRP activity by the appearance of a green coloured solution. The control experiment was performed using an equal concentration of HRP in the 100 mM pH 6 phosphate buffer solutions under the same conditions.

The activity of ALP was determined by measuring release of phosphate ions from pyrophosphate solutions [27]. 5 mL of each pyrophosphate concentration ranging from 0 to 20 mM was added to 5 mL of 1 U mL^{-1} ALP and then mixed. 160 μL of the pyrophosphate/ALP solution was sampled every 2 min during the reaction. Then, 330 μL of 5% trichloroacetic acid and 5 mM copper sulphate (Fisher scientific, Loughborough, UK) was added, following by the introduction of the colour reagents, containing 500 μL of 5% iron sulphate and 1% ammonium molybdate (Acros Organics, Loughborough, UK), and each sample was measured at 690 nm. All phosphate, pyrophosphate and ALP solutions were made in a 100 mM Tris–HCL buffer. Possible interference by phosphate release from the matrix was accounted for by measuring the phosphate concentration of the eluent in the absence of ALP.

Results

Following filtration using the water aspirated vacuum pump, the calcium phosphate-based material gelled to form a cylindrical sample, which when removed from the Büchner funnel exhibited sufficient mechanical integrity to retain its original geometry. After freeze drying, the resulting ACGs were shown to consist of a combination of apatite, as evidenced by a characteristic peak at 32° 2θ (Fig. 1), and calcite with peaks at 29°, 39°, 47°, 49° and 53° 2θ. The broadness of the peaks indicative of apatite suggests the formation of a poorly crystalline phase. The incorporation of either ALP or HRP into the ACG had no effect on the crystalline composition of the material (Fig. 1). FTIR spectra of the samples further confirmed that the incorporation of ALP or HRP into the ceramic matrix did not affect the composition of the material. Peaks present at 863, 1415 and 1479 cm^{-1} were indicative of the $v2$ and $v3$ vibrations of a carbonate ion. The presence of these vibrations could indicate either the presence of carbonate substitution of the apatite lattice or simply the presence of $CaCO_3$ in the sample. As expected, there were also peaks present at 561 and 1031 cm^{-1}, which were indicative of PO_4^{3-} vibrations (Fig. 2).

Although the addition of ALP and HRP to the ACGs had little influence of the true density of the material (Table 1),

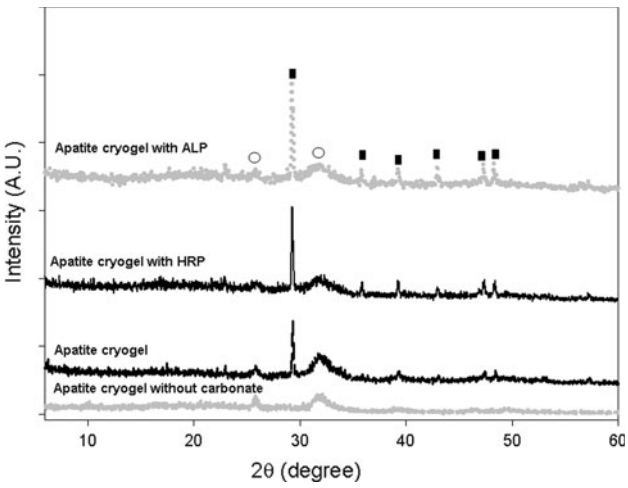

Fig. 1 X-ray diffraction patterns showing the influence of ALP or HRP addition on the crystalline compositions of the apatite cryogels and the addition of carbonate

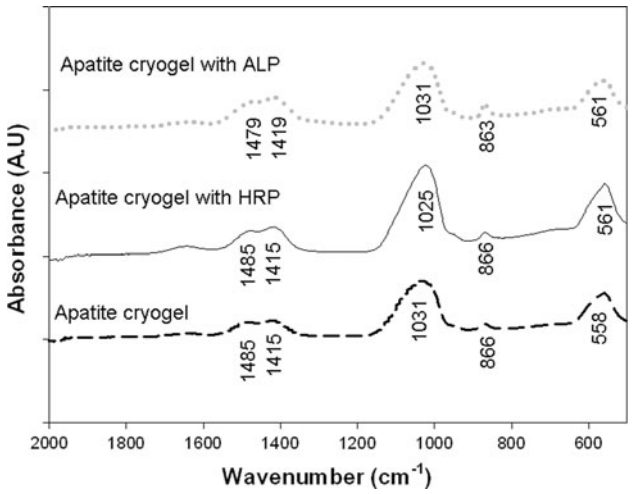

Fig. 2 FTIR spectra of the apatite cryogels, with and without the addition of ALP or HRP. The addition of either enzyme to the material during processing had little or no influence on the final composition of the material

each true density was significantly lower (2.5–2.6 g cm^{-3}) than would be expected for calcite (2.71 g cm^{-3}) or apatite (3.16 g cm^{-3}). This may suggest the presence of an X-ray amorphous phase of lower true density than either of these minerals. The incorporation of the enzymes into the ACGs resulted in a slight difference in the specific surface area exhibited by the gel material. The control material exhibited a specific surface area of 48.3 ± 4.6 m^2 g^{-1}, whereas the ACG formed in the presence of HRP exhibited a specific surface area of 53.12 ± 1.48 m^2 g^{-1} (Table 1), the specific surface area of the ACG containing ALP was lower than either other material (42.62 ± 1.55 m^2 g^{-1}); although this difference could be attributed to variations between different batches of the material. The incorporation of the enzymes into the ACG matrix also resulted in a reduction in the total porosity of the final material from 78 ± 3% for the control ACG to 57 ± 1% for the ACG containing HRP (Table 2), but a slight increase in the case of the ALP-loaded material (88 ± 3%). The reduction in the porosity that was exhibited by the ACG was accompanied by a reduction in the mean pore diameter exhibited by the material from 42 ± 28 nm, in the case of the control material, to 11 ± 1 nm following the addition of HRP to the material during processing (Table 2). The addition of ALP to the ACG resulted in a slightly increase in the mean pore diameter of the material to 44 ± 2 nm, following dispersion in double distilled water, the particle size of the precipitate was in the order of 400–600 nm in all processing conditions (Table 1). The crystallite size was shown to be significantly smaller than the particle size of the precipitate, which consisted of blade-like crystals of 100–150 nm in length and 20–30 nm in width (Fig. 3a). Examination of the surface of the ACG illustrated the presence of very few surface features as may be expected for a mesoporous cryogel material (Fig. 3b).

Once immersed in the elution medium, there was a burst release of HRP with 36 wt% of the enzyme released from the ceramic matrix within 1 day (Fig. 4). After 1 day of ageing, the rate of release from the matrix slowed so that over a period of 8 days of ageing only a further 8 wt% of the HRP was released into solution. In contrast, there was only a small release of ALP during the first day of ageing (10 wt%), with only 15 wt% of the ALP being released over a period of 8 days in solution (Fig. 4).

The activities of the encapsulated enzymes were evaluated over a period of 14 days of ageing. In the case of the HRP, activity was expressed in terms of the rate of $ABTS^+$ production per minute. When free in solution, the rate of conversion of the ABTS to $ABTS^+$ varied little and after 14 days of ageing, the HRP exhibited a rate of $ABTS^+$

Table 1 The true density, specific surface areas and particle sizes exhibited by the apatite from which the ACG was formed following precipitation in the absence of enzymes, in the presence of HRP and in the presence of ALP

	True density (g cm^{-3})	Specific surface area (m^2 g^{-1})	Particle size (nm)
Apatite cryogel (ACG)	2.35 ± 0.02	48.33 ± 4.60	536 ± 124
ACG + HRP	2.53 ± 0.03	53.12 ± 1.48	618 ± 17
ACG + ALP	2.59 ± 0.19	42.62 ± 1.55	436 ± 97

Table 2 The influence of protein addition on the microstructure of the ACG, including the total porosity, mean pore area and mean pore diameter

	Total pore area (m2 g^{-1})	Mean pore diameter (nm)	Porosity (%)
Apatite cryogel (ACG)	59 ± 8	42 ± 28	78 ± 3
ACG + HRP	60 ± 8	11 ± 1	39 ± 25
ACG + ALP	74 ± 2	44 ± 2	88 ± 3

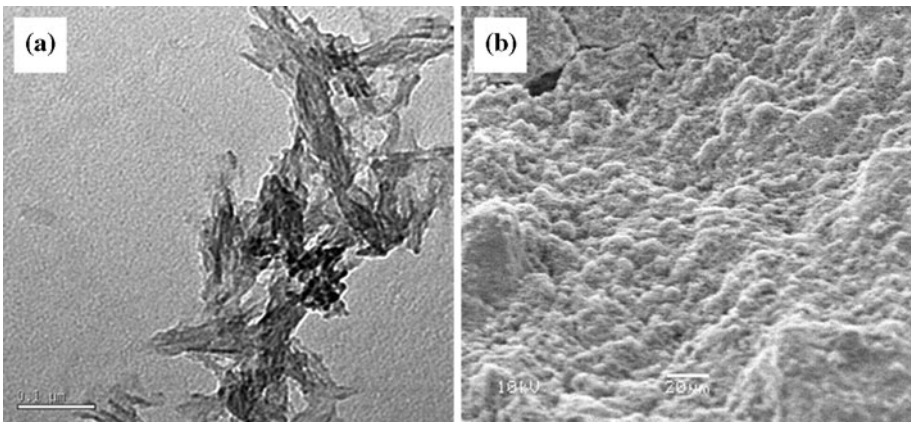

Fig. 3 Electron micrographs showing **a** the morphology of apatite crystallites dispersed in water prior to gel formation and **b** the surface of an apatite cryogel following processing

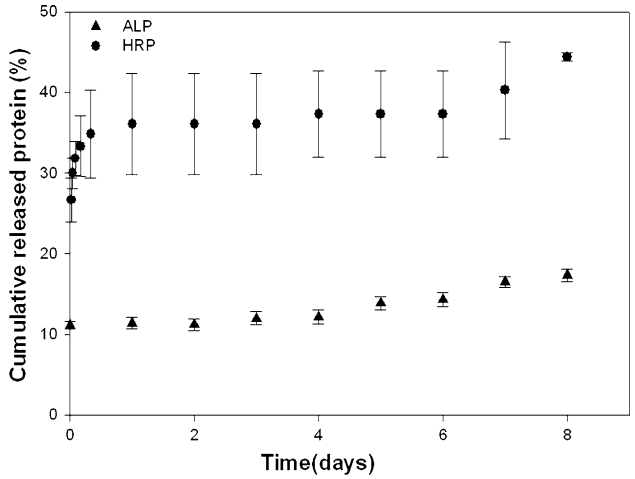

Fig. 4 The release of ALP or HRP from the ACG over a period of 10 days of ageing. There was an initial burst release of HRP from the matrix, followed by a plateau, whereas in the case of the ALP, after the first day of ageing, there was little further release from the apatite matrix

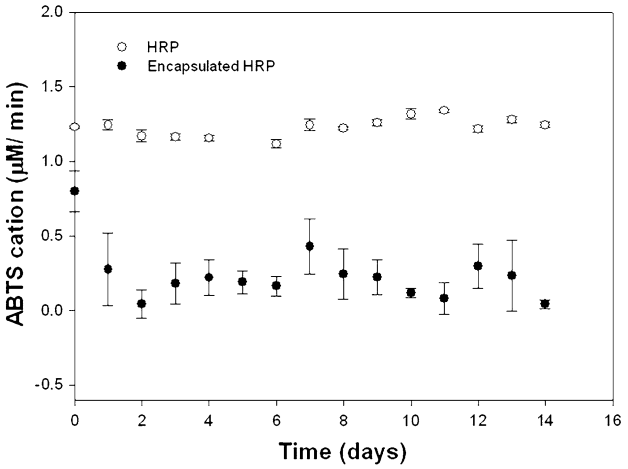

Fig. 5 The activity of HRP, expressed as the rate of production of $ABTS^+$ with time, free in solution and encapsulated within the ACG matrix. Encapsulation significantly reduced the rate of $ABTS^+$ production, when compared with the HRP free in solution

production of 1.2 μM min^{-1} (Fig. 5). The production of $ABTS^+$ catalysed by the encapsulated HRP was reduced from 0.8 to 0.1 μM min^{-1} after 2 days as shown in the Fig. 5. This reduction corresponded with the rapid release of the surface bound enzyme. After this time point, the $ABTS^+$ was produced at the rate of 0.22 μM min^{-1}. To investigate whether this reduction in activity could be attributed to mass transport limitations imposed by the presence of the gel, following 14 days of ageing the gel was crushed and the HRP released by EDTA, and quantified by the BCA assay. After release from the gel, the rate of $ABTS^+$ production increased to 0.8 μM min^{-1} (results not shown).

The activity of ALP was assessed by the hydrolysis of pyrophosphate ions and was expressed as μM min^{-1} (Fig. 6). The rate of phosphate production was higher at all time points for the encapsulated ALP than for the ALP that was free in solution. In the case of the free ALP, the rate of phosphate production could not be measured following 6 days of ageing. In comparison, phosphate production could be measured for a period of 12 days following encapsulation. All reported data were zeroed against the amount of phosphate eluted into the ageing medium in the absence of the ALP.

Discussion

The first successful encapsulation of a functional enzyme was reported by Braun et al. in 1990 [24]. The potential for this system to act as a molecular biosensor was well recognised and consequently there have since been numerous reports of silica gels being used to entrap enzymes such as HRP and ALP, as well as a host of other proteins [2, 25, 28]. Whilst silica gels have numerous advantages over other encapsulation technologies, such as their chemical inertness and ease of synthesis in ambient

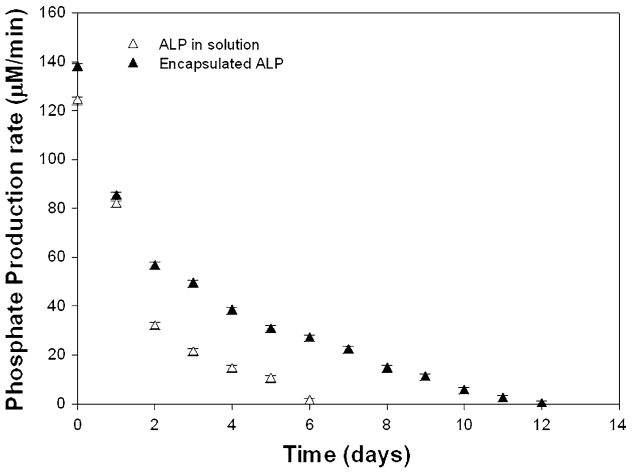

Fig. 6 The pyrophosphatase activity of the encapsulated and unencapsulated ALP over a period of 12 days ageing. Encapsulation was shown not to have a detrimental influence on the rate of phosphate production and also seemed to prolong the period of time during which the activity of the enzyme was measurable

conditions, the use of TMOS/TEOS in their fabrication leads to the formation of methanol or ethanol, which can compromise enzyme activity. Indeed, a previous study has shown that when incorporated into carbonated hydroxyapatite layers on 45S5 bioactive glasses, the enzymes exhibited comparatively low activities and when encapsulated within silica gel layers, activity was completely lost [29].

Since they are well tolerated in vivo and can form an intimate bond with both hard and soft tissues, calcium phosphate-based ceramics such as hydroxyapatite, β-tricalcium phosphate (β-TCP) and biphasic calcium phosphate are widely used for the replacement of hard tissues. Numerous researchers have investigated the efficacy of these materials for the delivery of therapeutic molecules such as vancomycin, ibuprofen-lysine and indomethacin [30–32]. Few studies, however, have investigated the ability of hydroxyapatite to encapsulate enzymes. There has recently been significant interest surrounding the immobilisation of ALP onto polymeric materials [33]. This study has been inspired by the increased understanding of the role of ALP in bone formation. ALP is found throughout the body in five different isoenzymes (intestinal, kidney, placental, tissue non-specific, germ cell). Tissue non-specific ALP (TNAP) is present in high concentrations on the surface of the cells responsible for depositing new bone matrix (osteoblasts) and in the matrix vesicles from which apatite crystals are deposited [21]. Its function in bone mineralisation is to remove an inhibitor to hydroxyapatite precipitation ($P_2O_7^{4-}$) to form PO_4^{3-} resulting in localised supersaturation and therefore precipitation [34]. It has also recently been shown that TNAP can act on amorphous calcium polyphosphate particles [35], which have been found in newly mineralising tissue and are thought to provide 'phosphate reservoirs' to enable new bone formation. By locally increasing ALP concentration in an implant, therefore, it may be possible to reduce the local $P_2O_7^{4-}$ to PO_4^{3-} ratio and thereby stimulate new bone deposition. This effect has been shown to be effective in vitro by enhancing the extent of mineralisation in osteoblast cultures [34]. Whilst some success has been noted, surface immobilisation of ALP can result in the interference of enzyme function through interaction with the plethora of other proteins and enzymes found in the body [36]. The mesoporous apatite gel reported here enables immobilisation and subsequent protection from other macromolecules. Over the period of study, the ACG was shown to retain 85 wt% of the loaded ALP (Fig. 4), which was comparable with the reported loading efficiency of gels loaded using non-surfactant template sol–gel processes [37]. Furthermore, encapsulation of the ALP enhanced the stability of the enzyme when compared with that left free in solution.

Whilst the ACG encapsulated and preserved the activity of the ALP, such success was not demonstrated for encapsulation of the HRP (Figs. 4 and 5). In comparison, the ACG encapsulated the HRP with a relatively low efficacy (66 wt%) and the activity of the encapsulated enzyme was significantly diminished when compared with that stored free in solution. Up to 1 day after encapsulation, the activity of the HRP was considerably higher than at any additional time-point. The relatively high activity at this point could be attributed to surface adsorbed HRP and the HRP that was released in a burst from the matrix on the first day. After this point, the activity of the enzyme was considerably reduced. The most likely reason for the reduction in activity on encapsulation could be poor mass transport through the mesoporous pore network in the cryogel, hindering the access of the substrate to the enzyme's active site [4, 38, 39]. This hypothesis was confirmed by the increase in $ABTS^+$ production once released from the ceramic matrix at the end of the study. The activity of the ALP may not have been influenced by the mesoporous pore network since the substrate of the reaction, the pyrophosphate anion (Mr = 174), is significantly smaller than ABTS (Mr = 514.62). Furthermore, the pyrophosphate anion [40] is well known to have a high affinity for calcium phosphate salts and as such is likely to have more rapidly perfused the ACG and attached strongly to the surface of the apatite. Charge may also have played a role in preventing mass transport of the $ABTS^+$ through the calcium phosphate-based matrix. The positive charge exhibited by the surface of the ACG may have prevented permeation of the transport of the $ABTS^+$ through the matrix. Indeed, electrostatic repulsion has previously been shown to have a significant influence on the catalytic efficacy of HRP [2].

The encapsulation of both proteins within the ACG seemed to have an influence on the microstructure of the gel. Whilst the incorporation of HRP into the ACG matrix reduced the mean pore diameter of the matrix by half, the addition of ALP during processing increased the mean pore diameter to 44 nm (Table 2). This change in microstructure could most likely be attributed to the incorporation of a significantly higher mass of ALP into the ACG than HRP, due to the lower activity of the ALP when compared with the HRP. The fluctuations in the specific surface area exhibited by the ACGs could also be attributed to the use of relatively high masses of ALP. Importantly, although the ALP altered the pore size distributions exhibited by the material, this did not detrimentally affect the ability of the ACG to store the enzyme. The addition of both proteins to the ACG during processing did not seem to influence the chemistry of the material. Interestingly, however, the strut densities exhibited by the gels were considerably lower than one might expect for gels consisting predominantly of apatite ($\rho = 3.16$ g cm^{-3}) and $CaCO_3$ ($\rho = 2.71$ g cm^{-3}) (Table 1). This may suggest the presence of an amorphous phase that was undetectable using XRD. It is possible that a metastable calcium phosphate phase of relatively low density such as brushite ($\rho = 2.32$ g cm^{-3}) was formed in the matrix during processing.

Conclusion

Here we report the successful encapsulation of ALP within a calcium phosphate-based gel matrix. The ACG immobilised 85 wt% of the ALP for the duration of the experiment and preserved enzyme activity when compared with the ALP that was free in solution. Evaluation of the ACG structure demonstrated that the material consisted in the most part of apatite and calcium carbonate with the presence of a comparatively low density phase that was undetectable using X-ray diffraction. Future work will seek to evaluate the efficacy of the material for stimulating bone formation in osteoblast cultures.

Acknowledgements The DVS and mercury porosimeter used in this research was obtained, through Birmingham Science City: Innovative Uses for Advanced Materials in the Modern World (West Midlands Centre for Advanced Materials Project 2), with support from Advantage West Midlands (AWM) and part funded by the European Regional Development Fund (ERDF).

References

1. Jin W, Brennan JD (2002) Anal Chim Acta 461:1
2. Kadnikova EN, Kostić NM (2002) J Mol Catal 18:39
3. Radin S, Ducheyne P, Kamplain T et al (2001) J Biomed Mater Res 57:313
4. Bhatia RB, Brinker CJ, Gupta AK, Singh AK (2002) Chem Mater 12:2434
5. Masahiro F, Kumi S, Kaoru H et al (2007) J Biomed Mater Res 81A:103
6. Lin T-Y, Wu C-H, Brennan JD (2007) Biosensors Bioelectron 22:1861
7. Wang G, Xu J-J, Chen H-Y, Lu Z-H (2003) Biosensors Bioelectron 18:335
8. Voss R, Brook MA, Thompson J et al (2007) J Mater Chem 17:4854
9. Miller SA, Hong ED, Wright D (2006) Macromol Biosci 6:839
10. Kitsugi T, Nakamara T, Oka M et al (1995) Calcif Tissue Int 57:155
11. Appleford MR, Oh S, Oh N et al (2009) J Biomed Mater Res A 89A:1019
12. Kitsugi T, Yamamuro T, Nakamura T et al (1993) Biomaterials 14:216
13. Brown WE, Chow LC (1983) J Dent Res 62:672
14. Ruhé PQ, Kroese-Deutman HC, Wolke JGC et al (2004) Biomaterials 25:2123
15. Kroese-Deutmana HC, Ruhé PQ, Spauwen PHM et al (2005) Biomaterials 26:1131
16. Otsuka M, Nakahigashi Y, Matsuda Y et al (1994) J Pham Sci 83:1569
17. Bohner M, Lemaître J, Van Landuyt P et al (1997) J Pham Sci 86:565
18. Barralet JE, Aldred S, Wright AJ et al (2002) J Biomed Mater Res 60:360
19. Nishioka T, Tomatsu S, Gutierrez MA et al (2006) Mol Gel Metab 88:244
20. Beortsen W, van den Bos T (1992) J Clin Invest 89:1974
21. Hessle L, Johnson KA, Anderson HC et al (2002) PNAS 99:9445
22. Bernhardt A, Lode A, Boxberger S et al (2008) J Mater Sci Mater Med 19:269
23. Anderson HC, Sipe JB, Hessle L et al (2004) Am J Pathol 164:841
24. Braun S, Rappoport S, Zusman R et al (1990) Mater Lett 10:1
25. Frenkel-Mullerad H, Avnir D (2005) J Am Chem Soc 127:8077
26. Wang Y, Caruso F (2005) Chem Mater 17:953
27. Xu Y, Cruz T, Pritzker P (1991) J Rheumatol 18:1606
28. Nicoll SB, Radin S, Santost EM et al (1997) Biomaterials 18:853
29. Lobel KD, Hench LL (1998) J Biomed Mater Res 39:575
30. Palazzo B, Sidoti MC, Roveri N et al (2005) Mater Sci Eng C 25:207
31. Xu QG, Tanaka Y, Czernuszka JT (2007) Biomaterials 28:2687
32. Gbureck U, Vorndran E, Barralet JE (2008) Acta Biomater 4:1480
33. Filmon R, Baslé MF, Atmani H, Chappard D (2002) Bone 30:152
34. Osathanon T, Giachelli CM, Somerman MJ (2009) Biomaterials 30:4513
35. Omelonl S, Georgiou J, Henneman ZJ et al (2004) PLoSONE 4:1
36. Boyan BD, Sylvia VL, Dean DD et al (1996) Connect Tissue Res 35:63
37. Wei Y, Xu J, Feng Q, Dong H, Lin M (2000) Mater Lett 44:6
38. Silva RA, Carmona-Ribeiro AM, Petri DFS (2007) Int J Biol Macromol 41:404
39. Jain TK, Rov I, De TK, Maitra A (1998) J Am Chem Soc 120:11092
40. Fleisch H, Bisaz S (1962) Nature 195:911